catalysts

MDPI

Article

Promoting Role of Bismuth on Hydrotalcite-Supported Platinum Catalysts in Aqueous Phase Oxidation of Glycerol to Dihydroxyacetone

Wenjie Xue [1], Zenglong Wang [1], Yu Liang [1], Hong Xu [1], Lei Liu [1,*] and Jinxiang Dong [1,2]

[1] College of Chemistry and Chemical Engineering, Taiyuan University of Technology, Taiyuan 030024, China; xuewenjie93@163.com (W.X.); wangzenglong1988@hotmail.com (Z.W.); lllyyy222666@163.com (Y.L.); xuhongwork@126.com (H.X.); dongjinxiangwork@hotmail.com (J.D.)

[2] School of Chemical Engineering and Light Industry, Guangdong University of Technology, Guangzhou 510006, China

* Correspondence: liulei@tyut.edu.cn; Tel.: +86-351-611-1178

Received: 16 December 2017; Accepted: 9 January 2018; Published: 11 January 2018

Abstract: Bismuth plays important roles in promoting the oxidation of alcohols towards high-value-added chemicals over a noble metal loading catalyst. Herein, Mg–Al hydrotalcite-supported platinum–bismuth nanoparticles (Pt–Bi/HT) were prepared by the co-impregnation method and used in the selective oxidation of glycerol towards dihydroxyacetone (DHA). The incorporation of Bi species into Pt/HT significantly enhances the conversion of glycerol and the selectivity of DHA. The high selectivity of DHA with 80.6% could be achieved at 25.1% conversion of glycerol. The Bi species of the Pt–Bi/HT catalyst mainly exist in the form of BiOCl and Bi metal, which is different from the previous Pt–Bi based catalyst, confirmed by a combination of powder X-ray diffraction (XRD), X-ray photoelectron spectroscopy (XPS), and high-resolution transmission electron microscopy (HR-TEM). A plausible mechanism is proposed to elucidate the promoting role of Bi species on the Pt/HT catalyst in the selective oxidation of glycerol towards DHA.

Keywords: Mg–Al hydrotalcite; platinum–bismuth nanoparticles; co-impregnation; glycerol oxidation; dihydroxyacetone

1. Introduction

Biodiesel, a well-known renewable biomass energy, can be produced by the transesterification of vegetable oils, waste oils, and animal fats with short chain alcohols; however, glycerol (GLY), as an inevitable byproduct, is abundantly obtained during the production of biodiesel [1]. As a result, the rapidly rising biodiesel production has led to a drastic surplus of GLY. The biodiesel-derived glycerol, as a potential platform molecule, could be converted into value-added chemicals by employing different chemical reactions [2–5], such as oxidation, hydrogenolysis, dehydration, and esterification. Much work in the past few years has been focused on the design of solid catalysts to catalyze the conversion of GLY into more valuable chemicals.

Glycerol oxidation could produce various high-value fine chemicals [6,7], such as dihydroxyacetone (DHA), glyceric acid, glyceraldehyde, and hydroxypyruvic acid. Platinum and gold catalysts are found to be the most active among the investigated catalysts for glycerol oxidation, and carbons (active carbon and carbon nanotubes, etc.) [7–9] and metallic oxides (TiO_2, Al_2O_3, CeO_2, CuO, MgO, $MgAl_2O_4$, etc.) [7,10–16] have been widely investigated as supports in previous studies. It has been found that the activity and product distribution are closely related to the support, especially the textural and chemical properties, and the acid–base property of the reaction medium; however, the main product was generally glyceric acid on mono-Pt and Au supported catalysts.

Among the products from the glycerol oxidation, DHA is one of the most interesting products owing to its wide application in cosmetics and the fine chemicals industry [3,7]. However, the poor selectivity for the desired product is a major issue for glycerol oxidation; such difficulty originates from the fact that the hydroxyl groups in glycerol show similar reactivity. Accordingly, careful designing of a catalyst is required to achieve high selectivity for DHA, which is derived from the oxidation of the secondary hydroxyl group of glycerol. The bismuth was firstly introduced to the Pt supported charcoal by Kimura and co-authors for the selective oxidation of glycerol in a batch reactor and a fixed-bed reactor in an acidic medium [17,18]. The bismuth as a promoter could significantly improve the selectivity of DHA—it was postulated that the bismuth as site blocker on the Pt (111) could control the glycerol orientation towards DHA formation. Recently, Hou's group succeeded in the selective oxidation of glycerol to DHA using a multiwall carbon nanotube (MWCNTs-) supported, Sb-promoted Pt catalyst, while the DHA yield was comparable to those using Pt–Bi catalysts [19]. In addition, a very few studies using Au-based catalysts have reported glycerol oxidation to DHA [7,16], but the DHA yield was generally less than that attained using Pt–Bi-based catalysts. Until now, most of the related studies have been devoted to optimizing Bi–Pt-based catalysts and corresponding reaction conditions in a neutral system [17–22]; the involved supports are mainly the carbon-based materials, such as active carbon [17,18,22], MWCNTs [19], and modified-carbon materials [20].

Mg–Al hydrotalcites (HTs) consist of positively charged Brucite-like layers ($Mg/Al(OH)_2$) with anionic species (i.e., OH^- and/or $HCO_3{}^-$) in the interlayer to form a neutral material. Mg–Al HT itself can be used as the catalyst for reactions associated with base-catalysis, and usually as a support to load the metal for many reactions [23,24]. Hydrotalcite-supported platinum nanoparticles (Pt NPs/HT) as a catalyst for the selective oxidation of glycerol have been reported in base-free aqueous [25,26], with glyceric acid as the main product. Recently, Wu's group reported the use of Mg–Al HT-hosted Cr(III) complex for the selective oxidation of GLY to DHA; the high selectivity for DHA (43.5%) was attributed to the synergistic effect between the chromium Schiff base complex and the weak base HT host [27]. For a Pt–Bi/charcoal catalyst for glycerol oxidation, it was found that the catalytic activity could be enhanced by increasing the pH value of the reaction medium, but the catalyst surface would be damaged by the solubilization of platinum at a high pH, leading to an obvious decrease in DHA selectivity [17,18].

In this work, Mg–Al hydrotalcite with weak alkalinity, which is different from the carbon-based materials, was used for the first time as a support to load Pt and Bi for the oxidation of glycerol to DHA. Pt–Bi/HT catalysts were characterized by XPS, HRTEM, and powder XRD. The catalytic performance and structural properties of Pt–Bi/HT were studied to understand the role of Bi in promoting DHA formation for Pt-based catalysts.

2. Results and Discussion

2.1. Catalyst Characterization

The successful preparation of Mg–Al hydrotalcite was confirmed by the powder XRD pattern comparison between the as-synthesized one and the standard Mg–Al HT, $Mg_4Al_2(OH)_{12}CO_3{\cdot}3H_2O$ (JCPD S541030), as shown in Figure 1. The SEM image of the as-synthesized Mg–Al HT sample (Figure S1) shows aggregates of small secondary uniform platelets of about 4 μm in diameter, and some secondary platelets could dissociate from the aggregates after loading the Pt–Bi species. Also, the powder XRD patterns for the Mg–Al HTs were collected after loading different amounts of Pt and Bi for phase identification. It can be seen that the characteristic peaks of HT are well preserved after loading Pt and Bi, suggesting that the typical layered structure of HT remains intact for all Pt–Bi supported HTs. The characteristic peaks of metallic Pt at 39.8°, 46.2°, and 67.5° and metallic Bi at 33.5°, 48.1°, and 59.8° were not observed for the Pt–*x*Bi/HT samples, indicating that high dispersions of Pt and Bi on the HT support were achieved and also revealed by TEM images (Figure 2). However, the characteristic peaks of BiOCl (Figure 2) could be clearly found on the Pt–Bi/HTs upon the Bi

loading above 1 wt % and the diffraction peak intensity for BiOCl gradually increases as the Bi content on the support increases. The species of BiOCl on the support are derived from the hydrolysis of $BiCl_3$ during the metal loading procedure. BiOCl could not be completely reduced to zero-valence Bi by $NaBH_4$, as was confirmed by XPS. It should be noted that Bi species generally existed in the form of $Bi_2O_2CO_3$ or Bi_2O_3 and Bi (0) meal for Pt–Bi-based catalysts [17–20], to which the hydrochloric acid was applied to improve the solubility of $BiCl_3$ during the Bi loading process. For Pt–Bi/HT catalysts in our study, the Bi loading procedure was carried out in the absence of hydrochloric acid with $BiCl_3$ as precursor of Bi, that maybe leads to the hydrolysis of $BiCl_3$ to BiOCl.

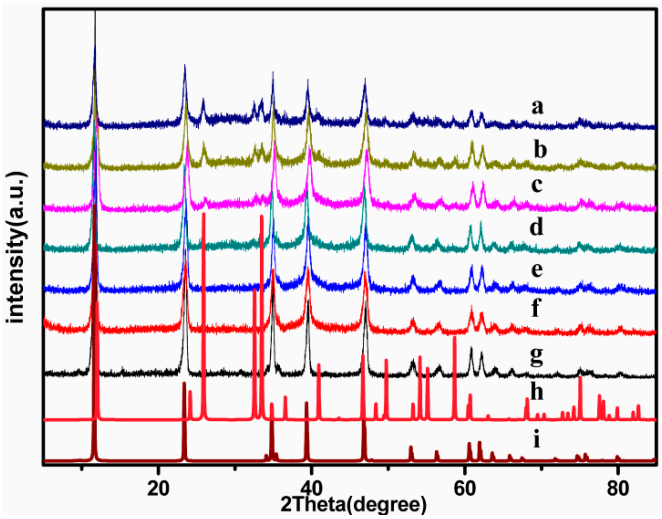

Figure 1. Powder XRD patterns of (**a**) Pt–9Bi/HT, (**b**) Pt–7Bi/HT, (**c**) Pt–5Bi/HT, (**d**) Pt–3Bi/HT, (**e**) Pt–1Bi/HT, (**f**) Pt/HT, (**g**) HT, (**h**) BiOCl, (**i**) $Mg_4Al_2(OH)_{12}CO_3{\cdot}3H_2O$. HT: hydrotalcite.

The morphology and distribution of Pt and Bi species on the surface of HT were observed by TEM images for various catalysts, as shown in Figure 2a,b. For the Bi-free Pt/HT, platinum nanoparticles with a mean diameter of 2.3 nm dispersed uniformly on the HT surface, suggesting that Mg–Al hydrotalcite with weak basicity is beneficial to improving the dispersion degree of Pt nanoparticles [26]. After loading Bi species, it could be observed that the nanoparticles with uniform dispersion were still preserved for the Pt–Bi/HT with various Bi contents, but the average diameter for the nanoparticles gradually increased with the increase of Bi content: 2.9 nm for Pt–3Bi/HT, 3.5 nm for Pt–7Bi/HT, and 4.2 nm for Pt–9Bi/HT. The increase in nanoparticle size upon the incorporation of Bi could possibly result from the formation of Pt–Bi species, in which the Pt nanoparticles were partly wrapped or covered by Bi-containing particles. The edge of Pt particles wrapped by a layer of Bi and BiOCl could be observed by HR-TEM image (Figure 2i,j). The *d*-spacing values of 0.196 and 0.224 nm correspond to those of the (200) and (111) planes for Pt metal [JCPDS 040802], respectively. The *d*-spacing value of 0.267 nm corresponds to that of the (110) plane of Bi metal [JCPDS 260214]. The *d*-spacing value of 0.275 nm corresponds to the (110) plane of BiOCl [JCPDS 060249], which fits well with that detected in XRD (Figure 1). The incorporation of Bi and BiOCl into the Pt/HT catalyst could also be confirmed by the XPS spectra, which contributes to the selective oxidation of glycerol to DHA with proper content of Bi species.

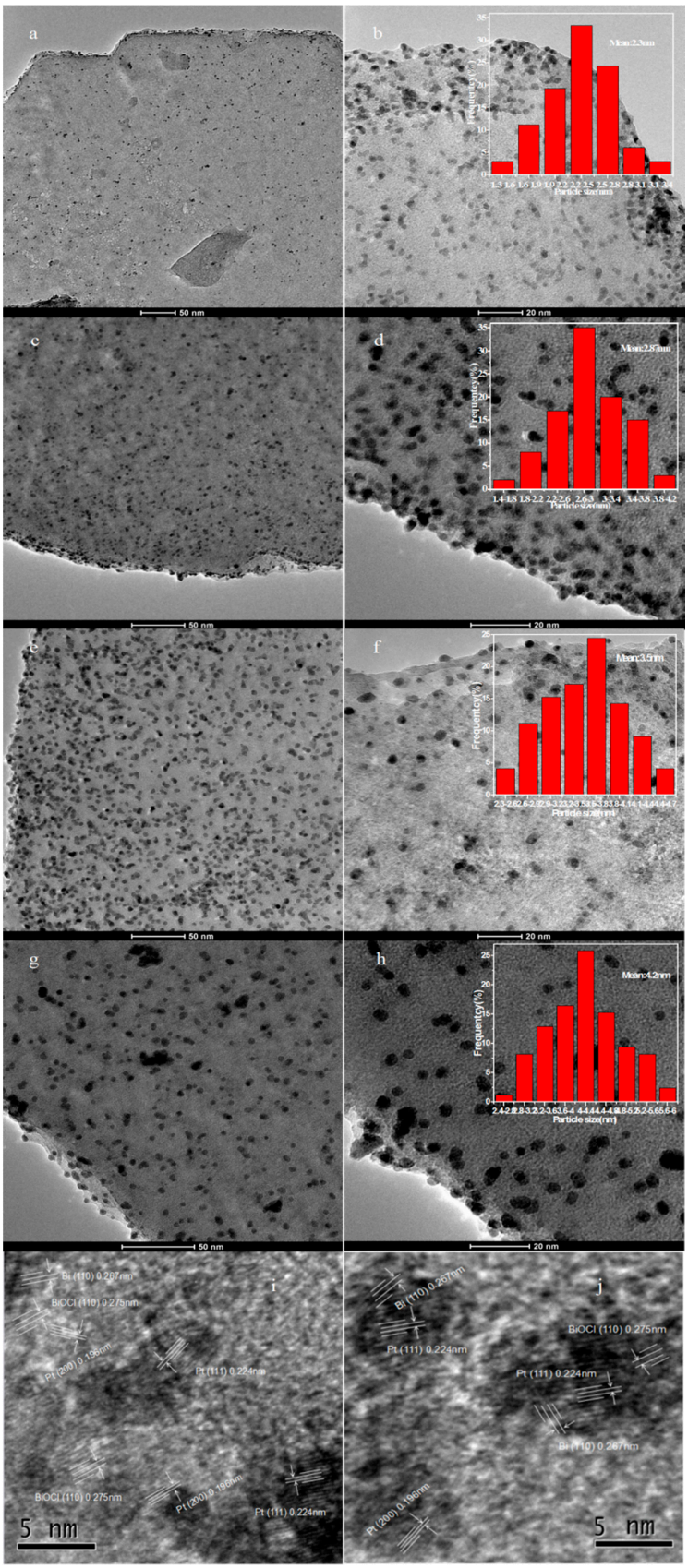

Figure 2. High-resolution TEM (HR-TEM) images and particle size distribution histograms for representative catalysts: (**a**,**b**) Pt/HT, (**c**,**d**) Pt–3Bi/HT, (**e**,**f**,**i**,**j**) Pt–7Bi/HT, and (**g**,**h**) Pt–9Bi/HT.

Figure 3 shows the N_2 adsorption–desorption isotherms for the as-synthesized HT and the typical catalysts after loading Pt–Bi species, which shows a type II hysteresis loop in the p/p_0 range of 0.8–1.0 according to the IUPAC classification. The BET surface area of HT decreased from 57.7 (micropore areas 14.8 m^2/g) to 36.5 m^2/g (micropore areas 1.0 m^2/g) after loading Pt onto the HT (Pt/HT catalyst). The incorporation of Pt into Pt/HT with different Bi content could not give rise to a significant change in BET surface area compared to Pt/HT with Pt loading alone—for example, 35.5 m^2/g for Pt–1Bi/HT and 34.6 m^2/g (micropore areas 0.9 m^2/g) for Pt–7Bi/HT. The reduction in micropore areas after metal loading could be possibly attributed to the disaggregation of aggregates consisting of secondary platelets (Figure S1) which contribute to the micropore systems, and the formation of platinum and Bi nanoparticles which blocks or fills the pore channel of the support, which is the case for the Pt supported on the porous supports [28,29].

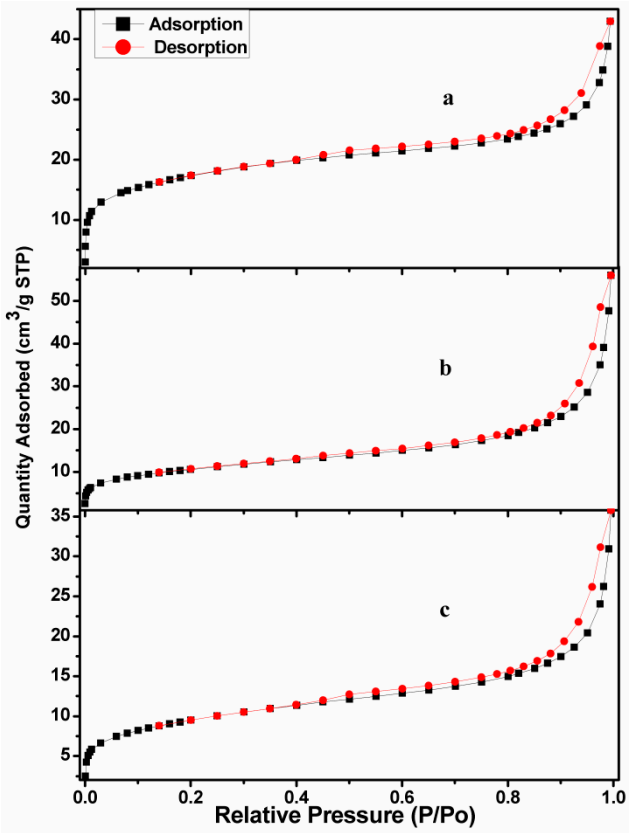

Figure 3. N_2 adsorption–desorption isotherms at 77 K for representative catalysts (**a**) HT, (**b**) 5%Pt–0%Bi/HT, (**c**) 5%Pt–7%Bi/HT.

XPS analysis was employed to study the chemical state and composition of Pt–Bi/HT catalysts. Figure 4 shows the deconvoluted Pt (4f), Bi (4f), and Cl (2p) XPS spectra for the representative Pt–7Bi/HT catalyst. The Pt 4f signal can be deconvoluted into two pairs of doublets and the XP lines arising from the Al 2p core level at 73.6–74.3 eV overlapped with those of the Pt. The most intensive doublet with binding energies of 70.8 (Pt 4f7/2) and 74.25 eV (Pt 4f5/2) is attributed to metallic Pt (0) [30]. The peaks located at 72.12 and 75.57 eV are assigned to Pt4f7/2 and Pt4f5/2, respectively, which is characteristic of the Pt (2+) ions of PtO in the achieved catalyst [31]. Based on the XPS analysis, the proportion of various chemical states for the detected Pt species could be concluded, consisting of 65.8% Pt (0) and 34.2% Pt (2+).

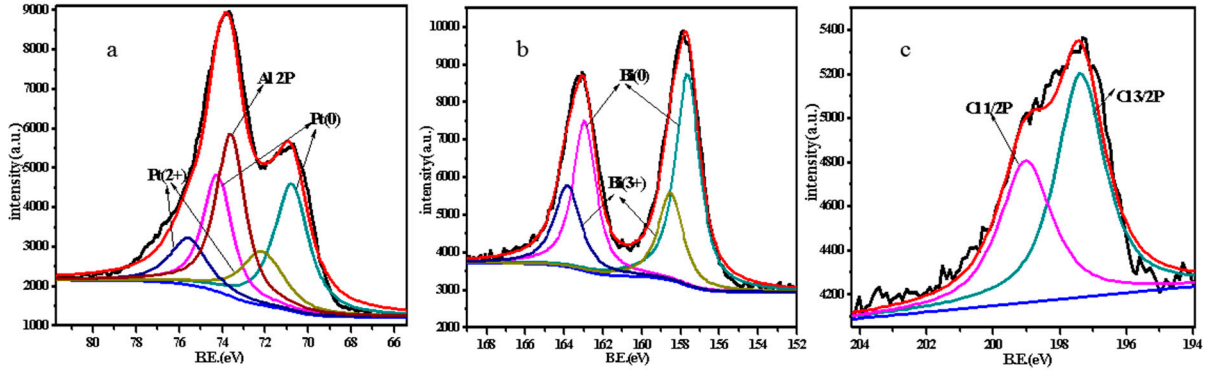

Figure 4. XPS spectra of Pt 4f (**a**), Bi 4f (**b**), and Cl 2P (**c**) in a typical Pt–7Bi/HT catalyst.

The XPS peak positions of Bi 4f show that the chemical states of Bi species mainly exist in the form of Bi (0) and Bi (3+) in the Pt–7Bi/HT catalyst, it this also the case for other Pt–Bi/HT catalysts in our study. The peaks at 156.7 and 163.0 eV are for the Bi 4f 7/2 and Bi 4f 5/2 region for Bi (0), respectively. The binding energy peaks located at 158.6 and 163.9 eV should be assigned to the Bi 4f 7/2 and Bi 4f 5/2 regions for BiOCl species [32]. In addition, the Cl 2p peak is deconvoluted into two peaks (198.2, 200.2 eV) corresponding to the Cl 2p 3/2 and Cl 2p 1/2 regions for BiOCl, respectively. The combination of XRD, TEM, and XPS analyses shows that the BiOCl species are formed on the surface of the HT support.

2.2. Catalytic Performance

2.2.1. Effect of Bi Content

To investigate the promoting role of Bi on a Pt-based HT catalyst, a series of Pt–Bi/HT catalysts with a constant Pt content of 5.0 wt % and different Bi content were prepared for glycerol oxidation with O_2 as the oxidant under atmospheric pressure; the catalytic reaction results are listed in Table 1. As can be seen from Table 1, the main products are DHA (38.3%) and glyceraldehyde (GLYALD) (38.8%) on the Pt alone supported on the HT catalyst with a low conversion ratio of 12.4%. Upon the incorporation of Bi species, including Bi metal and BiOCl confirmed by powder XRD, TEM, and XPS, a significant increase in catalytic activity and the selectivity of DHA was observed, and the selectivity of GLYALD obviously decreased from 38.8% to about 11%. A DHA selectivity of 80.6% could be achieved on the Pt–7Bi/HT catalyst with glycerol conversion at 25.1%. The selectivity of DHA is comparable to that (ca. 80%) observed on the Pt–Bi supported on carbon-based materials with high BET surface areas [19–22], in which Bi species were observed in the form of $Bi_2O_2CO_3$ or Bi_2O_3 and Bi meal, and the geometric blocking effect of active sites by bismuth adatoms was proposed for the high selectivity of DHA. Owing to the difference in Bi species among the Pt–Bi/HT and Pt–Bi/carbon-based materials, herein, the increase in catalytic activity and selectivity for DHA upon introduction of Bi species could be possibly attributed to the strong hydrogen bond between BiOCl on the surface of HT and glycerol molecule, which enormously enhances the adsorption ability of the catalyst towards glycerol. However, the catalytic activity decreases on the Pt–Bi/HT catalyst (Pt–9Bi/HT) with high loading of Bi species; this could possibly result from the severe wrapping of Pt nanoparticles by the Bi species which blocks glycerol access to the Pt active sites. The carbon monoxide adsorption amounts of Pt–7Bi/HT and Pt–9Bi/HT are 8.1 and 5.2 mL CO/g platinum, respectively, which coincides with their catalytic activity. The decrease in the CO adsorption amount is related to the wrapping and covering content of Pt nanoparticles by the Bi species incorporated into the catalysts. The edge of the Pt particles wrapped by a layer of Bi and BiOCl could also be observed by HR-TEM (Figure 2i,j).

Table 1. Catalytic reaction results on Pt–Bi/HT catalysts with various Bi contents [a].

Pt–*x*Bi/HT	Conversion (%)	Product Selectivity (%)							
		OA	TA	HYPAC	GLYAC	GLYALD	GLYCAC	DHA	AA
Pt/HT	12.4	0.2	0.4	0.0	11.8	38.8	5.7	38.3	4.8
Pt–1Bi/HT	21.5	2.6	2.1	5.5	9.3	11.4	0.8	68.0	0.3
Pt–3Bi/HT	21.0	2.0	1.8	5.4	8.4	11.8	0.7	69.6	0.3
Pt–5Bi/HT	27.3	1.9	2.1	5.4	7.9	11.9	1.0	69.7	0.1
Pt–7Bi/HT	25.1	1.1	2.0	2.0	2.9	10.6	0.7	80.6	0.1
Pt–9Bi/HT	19.5	1.8	1.6	4.0	7.5	11.4	0.7	73.0	0.0

[a] Reaction conditions: 0.1 g/mL glycerol aqueous solution 50 mL, catalyst 0.5 g, reaction temperature 70 °C, reaction time 6 h, O_2 flow rate 150 mL/min. (OA: oxalic acid; TA: tartronic acid; HYPAC: hydroxypyruvic acid; GLYAC: glycemic acid; GLYALD: glyceraldehyde; GLYCAC: glycolic acid; DHA: dihydroxyacetone; AA: acetic acid).

2.2.2. Effect of Reaction Temperature

The effect of reaction temperature on glycerol oxidation was investigated, and Table 2 summarizes the catalytic reaction results after a reaction time of 6 h over Pt–7Bi/HT. The glycerol oxidation reaction could not run at the reaction temperature of 30 °C. The glycerol conversion significantly increases with the increase of reaction temperature, and the selectivity of DHA attained the highest value of 80.6% with a glycerol conversion of 25.1% at 70 °C. At high reaction temperatures, the DHA product derived from the glycerol is further oxidized to other products, consequently leading to the decrease in DHA selectivity.

Table 2. Catalytic reaction results on Pt–Bi/HT catalysts at various reaction temperatures [a].

Temperature (°C)	Conversion (%)	Selectivity (%)							
		OA	TA	HYPAC	GLYAC	GLYALD	GLYCAC	DHA	AA
30	0.0	0.0	0.0	0.0	0.0	0.0	0.0	0.0	0.0
50	14.9	2.9	0.7	3.6	5.8	21.3	0.5	65.2	0.0
70	25.1	1.1	2.0	2.0	2.9	10.6	0.7	80.6	0.1
90	35.6	1.8	2.5	1.8	3.5	10.5	1.0	78.7	0.2

[a] Reaction conditions:0.1g/mL glycerol aqueous solution 50 mL, Pt–7Bi/HT catalyst 0.5 g, reaction time 6 h, O_2 flow rate 150 mL/min.

2.2.3. Effect of Reaction Time

The effect of reaction time on glycerol oxidation was studied over the Pt–7Bi/HT catalyst; the catalytic reaction results after different reaction times are summarized in Table 3. The catalytic activity of Pt–7Bi/HT gradually increases with the improvement of the reaction temperature, the DHA was the major product among the products of glycerol oxidation. However, the selectivity of DHA decreased to 62.4% at 12 h from 80.6% at 6 h, which can possibly be attributed to the over-oxidation of glycerol.

Table 3. Catalytic reaction results on Pt–Bi/HT catalysts at various reaction times [a].

Time (h)	Conversion (%)	Selectivity (%)							
		OA	TA	HYPAC	GLYAC	GLYALD	GLYCAC	DHA	AA
4	18.2	1.3	1.1	4.6	0.0	22.8	0.3	69.8	0.3
6	25.1	1.1	2.0	2.0	2.9	10.6	0.7	80.6	0.1
8	31.4	5.3	4.0	6.3	8.5	8.5	1.1	66.2	0.1
12	42.5	6.0	5.0	7.1	10.2	8.0	1.2	62.4	0.1

[a] Reaction conditions: 0.1 g/mL glycerol aqueous solution 50 mL, Pt–7Bi/HT catalyst 0.5 g, reaction temperature 70 °C, reaction time 6 h, O_2 flow rate 150 mL/min.

2.2.4. Catalyst Recycling

To determine the stability of Pt–Bi supported on an HT catalyst, three successive recycling experiments were carried out (Figure 5). After 6 h of reaction, the catalyst was centrifuged, washed with deionized water, dried under vacuum, and employed again for the next glycerol oxidation under identical conditions. It was observed that the conversion of glycerol decreased negligibly from 25.1% in the first run to 24.3% in the third run, and the selectivity of DHA had no obvious changes in the three successive runs. The powder XRD pattern of the second recycled catalyst (Figure S2) was identical to that of the initial catalyst, and the TEM images (Figure S3) show that there was no obvious change in the second recycled catalyst in particle size or particle size distribution. In addition, the used catalysts were separated from the reaction mixture and ICP measurements indicated that there was no leaching of Pt or Bi from the catalyst into solution during the reaction. Based on these results, the slight decrease in glycerol conversion could be attributed to the loss of catalyst during the recovery of the catalyst from the last run. These results suggested that the Pt–Bi/HT was stable and reusable as a catalyst for the selective oxidation of glycerol towards DHA.

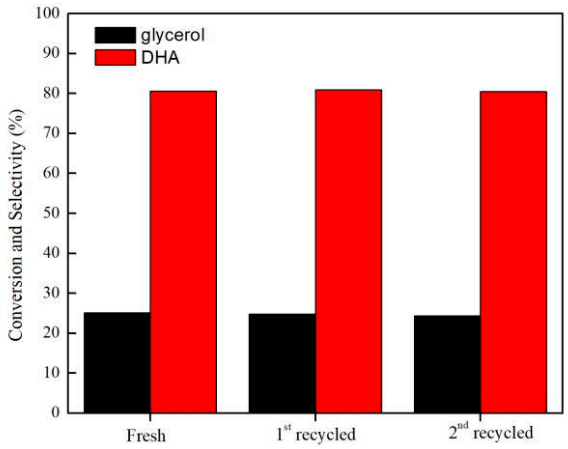

Figure 5. Recycling of Pt–7Bi/HT catalyst. Reaction condition: 0.1 g/mL glycerol aqueous solution 50 mL, Pt–7Bi/HT catalyst 0.5 g, reaction temperature 70 °C, reaction time 6 h, O_2 flow rate 150 mL/min.

2.2.5. Glycerol Selective Oxidation Mechanism

Although much work has shown that high selectivity can be achieved on Pt–Bi supported catalysts for the selective oxidation of alcohols, the origin of the promoting role of Bi on Pt-based catalysts still remains unclear. In the case of Pt–Bi-based catalysts used for the selective oxidation of glycerol towards DHA, three chemical states of Bi including Bi (0), Bi_2O_3, $Bi_2O_2CO_3$ and BiO(OH) [17–20] are often found. Various interpretations for the role of promoters, such as the geometric blocking effect of active sites [17,20,33] and the formation of a complex among Pt, Bi, and substrate [34], have been proposed. In this work, the Bi species on the Pt–Bi/ HT catalysts were observed in the form of Bi metal and BiOCl due to the slightly different preparation procedure, in which Bi loading was carried out in the absence of hydrochloric acid with $BiCl_3$ as precursor of Bi, showing that the catalyst preparation methods have an important effect on the composition and structure of catalysts and their catalytic performance [35]. Based on the previous mechanism and catalytic reaction results, a plausible model is proposed as shown in Figure 6 to elucidate the promoting role of Bi species on the Pt/HT catalyst in the selective oxidation of glycerol towards DHA. The promotional role of Bi species is dominated by the geometrical effect and the formation of strong hydrogen bonds between BiOCl on the surface of support and glycerol. The two terminal hydroxyl groups were bound on the surface of the Pt–Bi nanoparticles by the formation of a hydrogen bond between the Cl ion of BiOCl and the H of the primary –OH group of the glycerol molecule, and the bismuth adatoms' function as site blocker on the surface of the Pt metal to control glycerol orientation towards the oxidation of the secondary –OH

group. The weak electronic interaction between Pt and Bi could improve the catalytic activity through activating oxygen [36]; however, the hydrogen bond role between the BiOCl and glycerol could also work to some extent in the Pt–Bi/HT system.

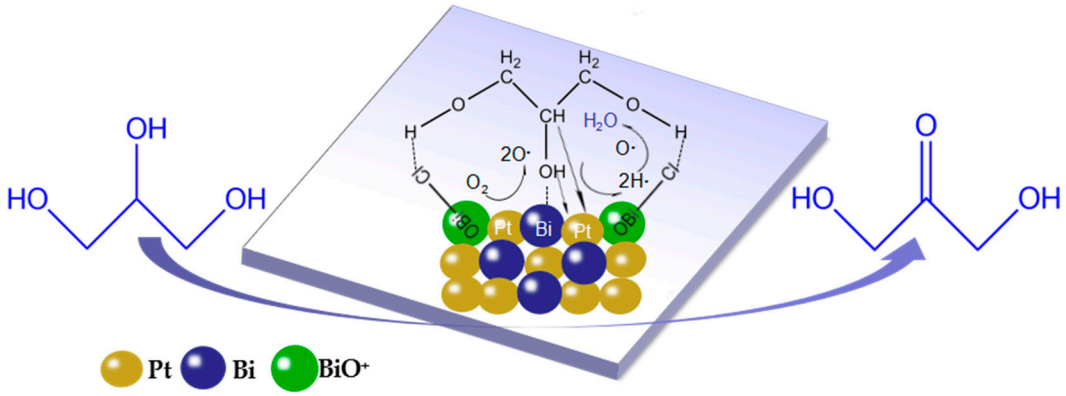

Figure 6. A proposed mechanism for the selective oxidation of glycerol towards DHA over the Pt–Bi/HT system.

3. Materials and Methods

3.1. Materials

Magnesium nitrate hexalydrate, aluminum nitrate nonahydrate, ureadihydroxyacetone dimer, glycolic acid, oxalic acid, formic acid, and acetic acid were obtained from Aladdin Industrial Corporation (Los Angeles, CA, USA). Hydroxypyruvic acid and DL-glyceraldehyde were purchased from Sigma-Aldrich Co., LLC (St. Louis, MO, USA). Glyoxylic acid and glyceric acid were obtained from Tokyo Chemical Industry (Tokyo, Japan). Tartronic acid was purchased from Alfa-Aesar (Haverhill, MA, USA), A Johnson Matthey Company (Royston, UK). Calcium mesoxalatetrihydrate, chloroplatinic acid hexahydrate, bismuth chloride, and $NaBH_4$ were purchased from J&KSEIENTIFIC Ltd. (Beijing, China). All the starting materials and solvents above were commercially available and used without further purification.

3.2. Catalyst Preparation

3.2.1. Synthesis of Hydrotalcite (HT)

The urea hydrolysis method was employed for the synthesis of Mg–Al hydrotalcite [37], wherein the urea is a weak Brönsted base, highly soluble in water, and the slow hydrolysis of urea enables the formation of Mg–Al HT with a small particle size and uniform morphology. Mg–Al hydrotalcite was hydrothermally synthesized from the mixture of $Mg(NO_3)_2{\cdot}6H_2O$, $Al(NO_3)_3{\cdot}9H_2O$, urea, and H_2O with a molar ratio of 4:1:12:333. The mixture was introduced into a Teflon-lined stainless steel auto-clave and placed in an oven at 100 °C for 24 h. The Mg–Al HT was obtained by filtration, washed with distilled water, and dried in an oven at 50 °C overnight. The obtained Mg–Al HT was directly used as a support for metal loading without calcination.

3.2.2. Metal Loading

Hydrotalcite-supported platinum and bismuth nanoparticle catalysts (Pt–*x*Bi/HT, x = 0, 1, 3, 5, 7, and 9) were prepared by the co-impregnation method, where x refers to the nominal weight percentage of Bi based on the support. First, a total of 93.3 mg of $H_2PtCl_6{\cdot}6H_2O$ and different amounts of $BiCl_3$ were dissolved in 20 mL of H_2O, and 700 mg of HT support was added to the above aqueous solution under stirring for 4 h; the suspension was heated to 100 °C under stirring to remove the water. Then, the obtained solid powder was added to 20 mL of fresh $NaBH_4$ aqueous solution (Pt and

$Bi/NaBH_4$ = 10 with mole ratio) and the solution was vigorously stirred for 30 min to reduce the Pt and Bi species. The resulting solid was recovered by filtration and washed thoroughly with distilled water. Finally, the gray-colored solid catalysts were obtained after drying in oven at 100 °C overnight. The Pt nominal loading was controlled at 5 wt % based on the HT support.

3.3. Characterization

The high-resolution transmission electron microscopy (HR-TEM) images were collected with a JEOL JEM-2010 (JEOL, Tokyo, Japan) electron microscope with an accelerating voltage of 120 kV. Powder X-ray diffraction (XRD) (Rigaku Corporation, Tokyo, Japan) patterns were recorded on a Rigaku MiniflexIIX-ray diffractometer with Cu Kα radiation (λ = 1.5418 Å) with a scan rate of 2°/min. N_2 adsorption–desorption experiments were carried out at 77 K (Micromeritics ASAP 2020 Instrument, Micromeritics, Atlanta, GA, USA) to determine the Brunauer–Emmett–Teller (BET) surface area and micropore volume. X-ray photoelectron spectroscopy (XPS) was obtained on a VG Milti Lab 2000 Spectrometer (Thermal VG, Waltham, MA, USA) with Al Kα radiation and a multichannel detector.

3.4. Catalytic Testing

The selective oxidation of glycerol was carried out in a 100 mL three-necked flask equipped with a reflux condenser and gas supply system. A total of 50 mL glycerol aqueous solution (0.1 g/mL) and 500 mg catalyst were put into the reactor, and heated to the required temperature (typically 60 °C) under stirring at 600 rpm, then O_2 was introduced into the reactor at 150 mL/min. After reaction, the reactor was quickly cooled down to room temperature with an ice bath, the catalyst was filtered off, and the aqueous solution was diluted 10 times with eluent before analysis. The reaction products were analyzed using a SHIMADZU LC-20AD HPLC (Shimadzu, Kyoto, Japan) equipped with UV detectors (210 nm) and a refractive index detector. An Aminex HPX-87H column (Bio-Rad, Hercules, CA, USA) was used for separation with a diluted H_2SO_4 (0.01 M) as eluent and a flow of 0.5 mL/min at 60 °C. The amount of glycerol and produced products were quantified with an external calibration method. The glycerol conversion and product selectivity were defined as follows:

$$\text{conversion} = \frac{\sum(\text{Mole of the product} \times \text{carbon number of the product})}{\text{Initial mole of glycerol} \times 3} \times 100\%,$$

$$\text{Selectivity} = \frac{\text{Mole of the product}}{\sum(\text{Mole of the product})} \times 100\%.$$

4. Conclusions

Mg–Al hydrotalcite-supported Pt–Bi nanoparticles with high dispersion were prepared by the co-impregnation method, and Pt–Bi/HT catalysts were found to be highly active and more efficient than Pt alone supported by HT towards the selective oxidation of glycerol to DHA in a base-free aqueous solution. The BiOCl and Bi metal are the main components of Bi species in the Pt–Bi/HT catalyst, and the Bi species have a significant role in promoting the conversion of glycerol and the selectivity of DHA. The promotional role of Bi species is dominated by the geometrical effect and the formation of strong hydrogen bonds between the Cl ion of BiOCl on the surface of support and the primary –OH group of the glycerol molecule. This work presented a new understanding on the promotional role of Bi species in the selective oxidation of glycerol towards DHA by noble metal loading catalysts.

Supplementary Materials: The following are available online at www.mdpi.com/2073-4344/8/1/20/s1, Figure S1: SEM images of the as-synthesized Mg–Al HT (left) and the Pt–7Bi/HT (right), Figure S2: Powder XRD patterns of (a) Pt–7Bi/HT catalyst after second reaction, (b) Pt–7Bi/HT fresh catalyst, Figure S3: HR-TEM images and particle size distribution histograms for Pt–7Bi/HT catalyst after second reaction.

Acknowledgments: This work was financially supported by the National Natural Science Foundation (21276174 and 21322608), Program for the Shanxi Young Sanjin Scholar, Program for the Innovative Talents of Higher Learning Institutions of Shanxi, and A Foundation for the Author of National Excellent Doctoral Dissertation of PR China (No. 201350).

Author Contributions: Lei Liu and Jinxiang Dong conceived and designed the experiments; Wenjie Xue and Zenglong Wang performed the experiments; Wenjie Xue and Jinxiang Dong analyzed the data; Wenjie Xue and Lei Liu wrote the paper; Yu Liang and Hong Xu helped perform the analysis with constructive discussions.

Conflicts of Interest: The authors declare no conflict of interest.

References

1. Quispe, C.A.; Coronado, C.J.; Carvalho, J.A., Jr. Glycerol: Production, consumption, prices, characterization and new trends in combustion. *Renew. Sustain. Energy Rev.* **2013**, *27*, 475–493. [CrossRef]
2. Zhou, C.H.C.; Beltramini, J.N.; Fan, Y.X.; Lu, G.M. Chemoselective catalytic conversion of glycerol as a biorenewable source to valuable commodity chemicals. *Chem. Soc. Rev.* **2008**, *37*, 527–549. [CrossRef] [PubMed]
3. Pagliaro, M.; Ciriminna, R.; Kimura, H.; Rossi, M.; Della Pina, C. From glycerol to value-added products. *Angew. Chem. Int. Ed.* **2007**, *46*, 4434–4440. [CrossRef] [PubMed]
4. Behr, A.; Eilting, J.; Irawadi, K.; Leschinski, J.; Lindner, F. Improved utilisation of renewable resources: New important derivatives of glycerol. *Green Chem.* **2008**, *10*, 13–30. [CrossRef]
5. Brandner, A.; Lehnert, K.; Bienholz, A.; Lucas, M.; Claus, P. Production of biomass-derived chemicals and energy: Chemocatalytic conversions of glycerol. *Top. Catal.* **2009**, *52*, 278–287. [CrossRef]
6. Katryniok, B.; Kimura, H.; Skrzyńska, E.; Girardon, J.S.; Fongarland, P.; Capron, M.; Dumeignil, F. Selective catalytic oxidation of glycerol: Perspectives for high value chemicals. *Green Chem.* **2011**, *13*, 1960–1979. [CrossRef]
7. Villa, A.; Dimitratos, N.; Chan-Thaw, C.E.; Hammond, C.; Prati, L.; Hutchings, G.J. Glycerol oxidation using gold-containing catalysts. *Acc. Chem. Res.* **2015**, *48*, 1403–1412. [CrossRef] [PubMed]
8. Liang, D.; Gao, J.; Sun, H.; Chen, P.; Hou, Z.; Zheng, X. Selective oxidation of glycerol with oxygen in a base-free aqueous solution over MWNTs supported Pt catalysts. *Appl. Catal. B* **2011**, *106*, 423–432. [CrossRef]
9. Carrettin, S.; McMorn, P.; Johnston, P.; Griffin, K.; Kiely, C.J.; Hutchings, G.J. Oxidation of glycerol using supported Pt, Pd and Au catalysts. *Phys. Chem. Chem. Phys.* **2003**, *5*, 1329–1336. [CrossRef]
10. Lakshmanan, P.; Upare, P.P.; Le, N.T.; Hwang, Y.K.; Hwang, D.W.; Lee, U.H.; Chang, J.S. Facile synthesis of CeO_2-supported gold nanoparticle catalysts for selective oxidation of glycerol into lactic acid. *Appl. Catal. A Gen.* **2013**, *468*, 260–268. [CrossRef]
11. Demirel-Gülen, S.; Lucas, M.; Claus, P. Liquid phase oxidation of glycerol over carbon supported gold catalysts. *Catal. Today* **2005**, *102*, 166–172. [CrossRef]
12. Villa, A.; Gaiassi, A.; Rossetti, I.; Bianchi, C.L.; van Benthem, K.; Veith, G.M.; Prati, L. Au on $MgAl_2O_4$ spinels: The effect of support surface properties in glycerol oxidation. *J. Catal.* **2010**, *275*, 108–116. [CrossRef]
13. Shen, Y.; Zhang, S.; Li, H.; Ren, Y.; Liu, H. Efficient synthesis of lactic acid by aerobic oxidation of glycerol on Au–Pt/TiO_2 catalysts. *Chem. Eur. J.* **2010**, *16*, 7368–7371. [CrossRef] [PubMed]
14. Xu, C.; Du, Y.; Li, C.; Yang, J.; Yang, G. Insight into effect of acid/base nature of supports on selectivity of glycerol oxidation over supported Au-Pt bimetallic catalysts. *Appl. Catal. B* **2015**, *164*, 334–343. [CrossRef]
15. Brett, G.L.; He, Q.; Hammond, C.; Miedziak, P.J.; Dimitratos, N.; Sankar, M.; Knight, D.W. Selective Oxidation of Glycerol by Highly Active Bimetallic Catalysts at Ambient Temperature under Base-Free Conditions. *Angew. Chem. Int. Ed.* **2011**, *50*, 10136–10139. [CrossRef] [PubMed]
16. Liu, S.S.; Sun, K.Q.; Xu, B.Q. Specific selectivity of Au-catalyzed oxidation of glycerol and other C_3-polyols in water without the presence of a base. *ACS Catal.* **2014**, *4*, 2226–2230. [CrossRef]
17. Kimura, H.; Tsuto, K.; Wakisaka, T.; Kazumi, Y.; Inaya, Y. Selective oxidation of glycerol on a platinum-bismuth catalyst. *Appl. Catal. A Gen.* **1993**, *96*, 217–228. [CrossRef]
18. Kimura, H. Selective oxidation of glycerol on a platinum-bismuth catalyst by using a fixed bed reactor. *Appl. Catal. A Gen.* **1993**, *105*, 147–158. [CrossRef]
19. Nie, R.; Liang, D.; Shen, L.; Gao, J.; Chen, P.; Hou, Z. Selective oxidation of glycerol with oxygen in base-free solution over MWCNTs supported PtSb alloy nanoparticles. *Appl. Catal. B* **2012**, *127*, 212–220. [CrossRef]

20. Ning, X.; Li, Y.; Yu, H.; Peng, F.; Wang, H.; Yang, Y. Promoting role of bismuth and antimony on Pt catalysts for the selective oxidation of glycerol to dihydroxyacetone. *J. Catal.* **2016**, *335*, 95–104. [CrossRef]
21. Xiao, Y.; Greeley, J.; Varma, A.; Zhao, Z.J.; Xiao, G. An experimental and theoretical study of glycerol oxidation to 1,3-dihydroxyacetone over bimetallic Pt-Bi catalysts. *AlChE J.* **2017**, *63*, 705–715. [CrossRef]
22. Hu, W.; Knight, D.; Lowry, B.; Varma, A. Selective oxidation of glycerol to dihydroxyacetone over Pt–Bi/C catalyst: Optimization of catalyst and reaction conditions. *Ind. Eng. Chem. Res.* **2010**, *49*, 10876–10882. [CrossRef]
23. Li, C.; Wei, M.; Evans, D.G.; Duan, X. Recent advances for layered double hydroxides (LDHs) materials as catalysts applied in green aqueous media. *Catal. Today* **2015**, *247*, 163–169. [CrossRef]
24. Zhou, L.; Shao, M.; Wei, M.; Duan, X. Advances in efficient electrocatalysts based on layered double hydroxides and their derivatives. *J. Energy Chem.* **2017**, *26*, 1094–1106. [CrossRef]
25. Tsuji, A.; Rao, K.T.V.; Nishimura, S.; Takagaki, A.; Ebitani, K. Selective Oxidation of Glycerol by Using a Hydrotalcite-Supported Platinum Catalyst under Atmospheric Oxygen Pressure in Water. *ChemSusChem* **2011**, *4*, 542–548. [CrossRef] [PubMed]
26. Tongsakul, D.; Nishimura, S.; Thammacharoen, C.; Ekgasit, S.; Ebitani, K. Hydrotalcite-supported platinum nanoparticles prepared by a green synthesis method for selective oxidation of glycerol in water using molecular oxygen. *Ind. Eng. Chem. Res.* **2012**, *51*, 16182–16187. [CrossRef]
27. Wang, X.; Wu, G.; Wang, F.; Ding, K.; Zhang, F.; Liu, X.; Xue, Y. Base-free selective oxidation of glycerol with 3% H_2O_2 catalyzed by sulphonato-salen-chromium(III) intercalated LDH. *Catal. Commun.* **2012**, *28*, 73–76. [CrossRef]
28. Zhu, S.; Gao, X.; Zhu, Y.; Li, Y. Promoting effect of WO_x on selective hydrogenolysis of glycerol to 1,3-propanediol over bifunctional Pt-WO_x/Al_2O_3 catalysts. *J. Mol. Catal. A* **2015**, *398*, 391–398. [CrossRef]
29. Feng, S.; Zhao, B.; Liu, L.; Dong, J. Platinum Supported on WO_3-Doped Aluminosilicate: A Highly Efficient Catalyst for Selective Hydrogenolysis of Glycerol to 1,3-Propanediol. *Ind. Eng. Chem. Res.* **2017**, *56*, 11065–11074. [CrossRef]
30. Bhogeswararao, S.; Srinivas, D. Catalytic conversion of furfural to industrial chemicals over supported Pt and Pd catalysts. *J. Catal.* **2015**, *327*, 65–77. [CrossRef]
31. Bhogeswararao, S.; Srinivas, D. Intramolecular selective hydrogenation of cinnamaldehyde over CeO_2–ZrO_2-supported Pt catalysts. *J. Catal.* **2012**, *285*, 31–40. [CrossRef]
32. Wang, C.; Shao, C.; Liu, Y.; Zhang, L. Photocatalytic properties BiOCl and Bi_2O_3nanofibers prepared by electrospinning. *Scr. Mater.* **2008**, *59*, 332–335. [CrossRef]
33. Kwon, Y.; Birdja, Y.; Spanos, I.; Rodriguez, P.; Koper, M.T. Highly selective electro-oxidation of glycerol to dihydroxyacetone on platinum in the presence of bismuth. *ACS Catal.* **2012**, *2*, 759–764. [CrossRef]
34. Mondelli, C.; Ferri, D.; Grunwaldt, J.D.; Krumeich, F.; Mangold, S.; Psaro, R.; Baiker, A. Combined liquid-phase ATR-IR and XAS study of the Bi-promotion in the aerobic oxidation of benzyl alcohol over Pd/Al_2O_3. *J. Catal.* **2007**, *252*, 77–87. [CrossRef]
35. Roy, I.; Bhattacharyya, A.; Sarkar, G.; Saha, N.R.; Rana, D.; Ghosh, P.P.; Palit, M.; Das, A.R.; Chattopadhyay, D. In situ synthesis of a reduced graphene oxide/cuprous oxide nanocomposite: A reusable catalyst. *RSC Adv.* **2014**, *4*, 52044–52052. [CrossRef]
36. Zhou, C.; Guo, Z.; Dai, Y.; Jia, X.; Yu, H.; Yang, Y. Promoting role of bismuth on carbon nanotube supported platinum catalysts in aqueous phase aerobic oxidation of benzyl alcohol. *Appl. Catal. B* **2016**, *181*, 118–126. [CrossRef]
37. Adachi-Pagano, M.; Forano, C.; Besse, J.-P. Synthesis of Al-rich hydrotalcite-like compounds by using the urea hydrolysis reaction—Control of size and morphology. *J. Mater. Chem.* **2003**, *13*, 1988–1993. [CrossRef]